biology

MDPI

Article

Uncovering the Regulatory Role of Proteins in EBSS-Induced Autophagy Using RNA-Seq Analysis

Chen Ruan [1,2,*], Yuzhu Li [3] and Ran Wu [4]

[1] Henan Key Laboratory of Industrial Microbial Resources and Fermentation, Technology School of Biological and Chemical Engineering, Nanyang Institute of Technology, Nanyang 473004, China
[2] School of Life Sciences, Huazhong University of Science and Technology, Wuhan 430074, China
[3] Technology School of Chemical and Pharmaceutical Engineering, Nanyang Normal University, Nanyang 473061, China; yzllyz19@163.com
[4] Technology School of Information Engineering, Nanyang Institute of Technology, Nanyang 473004, China; wuran@nyist.edu.cn
* Correspondence: 3131071@nyist.edu.cn; Tel.: +86-16696306458

Simple Summary

EBSS is a classical autophagy inducer that provides a special culture environment lacking amino acids and serum, causing cell starvation. However, there are almost no relevant omics data related to EBSS-induced autophagy, and consequently, autophagy-regulatory proteins have not been fully elucidated. In this study, we selected EBSS-induced autophagy as our research object and uncovered proteins that have regulatory roles in this process using RNA-seq analysis. Through the combination of omics calculation and biological experiments, this study has revealed, for the first time, that TXNRD1 has a regulatory function for autophagy activation in EBSS-induced autophagy. Our research provides useful omics information that contributes to the clarification of the autophagy mechanism.

Abstract

Earle's balanced salt solution (EBSS) is a classical autophagy inducer that provides a special culture environment lacking amino acids and serum, causing cell starvation. However, the production of relevant omics data surrounding EBSS-induced autophagy is still in the early stage. The objective of this study was to identify new potential functional proteins in the autophagy process through omics analysis. We selected EBSS-induced autophagy as our research object and uncovered autophagy-regulatory proteins using RNA-seq analysis. Western blotting showed that EBSS increased LC3B-II protein levels in NRK cells, reaching the maximum amount at 2 h of culture. Then, we used next-generation sequencing to obtain quantified RNA-seq data from cells incubated with EBSS and the bowtie–tophat–cufflinks flow path to analyze the transcriptome data. Using significant differences in the FPKM values of genes in the treated group compared with those in the control group to indicate differential expression, 470 candidate genes were selected. Subsequently, GO and KEGG analyses of these genes were performed, revealing that most of these signaling pathways were closely associated with autophagy, and to better understand the potential functions and connections of these genes, protein–protein interaction networks were studied. Considering all the conclusions of the analysis, 27 candidate genes were selected for verification, where the knockdown of *Txnrd1* decreased LC3B-II protein levels in NRK cells, consistent with the results of confocal experiments. In conclusion, we uncovered autophagy-regulatory proteins using RNA-seq analysis, with our results indicating that TXNRD1 may play a role in regulating EBSS-induced autophagy via an unknown pathway. We hope that our research can provide useful information for further autophagy omics research.

check for updates

Academic Editor: Maurizio Forte

Received: 22 August 2025
Revised: 26 September 2025
Accepted: 3 October 2025
Published: 8 October 2025

Citation: Ruan, C.; Li, Y.; Wu, R. Uncovering the Regulatory Role of Proteins in EBSS-Induced Autophagy Using RNA-Seq Analysis. *Biology* **2025**, *14*, 1373. https://doi.org/10.3390/biology14101373

Copyright: © 2025 by the authors. Licensee MDPI, Basel, Switzerland. This article is an open access article distributed under the terms and conditions of the Creative Commons Attribution (CC BY) license (https://creativecommons.org/licenses/by/4.0/).

Keywords: autophagy; EBSS; RNA-seq; NRK; Txnrd1

1. Introduction

Autophagy is a highly conserved, selective process of biodegradation in plants, animals and microbes [1], playing an important role in many physiological and pathological processes, such as nutritional deprivation, environmental stress, cancer and neurodegenerative diseases [2,3]. Many autophagy regulators have been identified as playing very important roles within the several autophagy types and signaling pathways in a multitude of studies. For example, the CDK7-CDK4 signaling axis potentiates SiNP-induced autophagy by phosphorylating RB1, thus activating E2F1 and FOXO3, with the help of autophagy-inducing nanoparticles [4,5].

A wide range of autophagy inducers have been discovered by researchers in the past. The classic autophagy inducer rapamycin inhibits the enzymatic activity of mechanistic target of rapamycin kinase (MTOR) to activate the downstream autophagy system [6]. Moreover, the class I PI3K pathway inhibitor N-acetyl-D-sphingosine, the inositol monophosphatase inhibitor carbamazepine and lithium chloride activate autophagy by inhibiting certain proteins and kinases that regulate autophagy [7]. EBSS, one of the first autophagy inducers that functions similarly to serum-free induction, provides a cell-starvation environment for the initial activation of autophagy in experiments, and scientists have found ATG proteins to have autophagy-regulatory activity in these conditions [8]; ATG16L has been found to interact with Apg5 and is closely related to the formation of autophagosomes [9]. Researchers have found numerous proteins that have regulatory functions in EBSS-induced autophagy, such as phosphatidylinositol 3-kinase, GORASP2 and p53 [10]. Until now, EBSS has primarily been used in experimental controls in the field of autophagy, with researchers using EBSS treatment as a control to ascertain whether autophagy flux is unobstructed in nanoparticle-induced autophagy [11].

In recent years, various omics technologies have been widely applied in the development of autophagy research. A multi-omics analysis study revealed the role of the autophagy-related gene AGT in chemotherapy resistance in colorectal cancer, with the gene mainly expressed in areas with malignant tumors and exhibiting distinct spatial characteristics [12]. In a recent study, protein modification omics demonstrated that LARS1 lactylation inhibits autophagy by activating mTORC1 [13]. The interaction network of the sole autophagy transmembrane protein atg9 has also been clarified with the help of the proteome and transcriptome [14]. However, there are almost no relevant omics data on the induction of autophagy by EBSS.

The objective of this study is to identify new potential functional proteins in the process of EBSS-induced autophagy through omics techniques. We selected normal rat kidney (NRK) epithelial cells as an in vitro model and applied next-generation sequencing to obtain quantified RNA-seq data on the cells when incubated with EBSS in an attempt to find new regulatory genes through bioinformatics analysis and molecular biology experimentation. We hope that our research provides useful information for autophagy omics research.

2. Materials and Methods

2.1. Reagents and Antibodies

EBSS was purchased from Procell Life Science & Technology (PB180334). Microtubule-associated protein 1 light chain 3 beta (LC3B) antibodies and β-actin (ACTB) antibodies were purchased from Proteintech Group (14600-1-AP and 18420-1-AP, Wuhan, China). Dulbecco's modified Eagle's medium (DMEM) and fetal bovine serum were purchased

from Procell Life Science & Technology (PM150210, Wuhan, China). The small interfering (si)RNAs were purchased from RiboBio (Guangzhou, China).

2.2. Cell Culture

The following describes the cell culturing process: Place the NRK cells stored in the liquid nitrogen tank into a constant-temperature water bath at 37 °C. Use forceps to continuously shake the cell storage tube to facilitate the rapid thawing of the cells. After the cells are thawed, disinfect the laminar flow hood with medical alcohol, transfer the cells to a 15 mL centrifuge tube, add DEME cell culture medium containing 10% FBS and mix thoroughly. Remove the supernatant, add another 5 mL of cell culture medium, and gently vortex to ensure thorough mixing. NRK cells were incubated in DMEM supplemented with 10% fetal bovine serum, 100 U/mL penicillin and 0.1 mg/mL streptomycin. The cells were cultured in a 37 °C and 5% carbon dioxide environment.

2.3. Starvation Inducement of Autophagy

When the cell confluence reaches approximately 90%, the cell culture stops. At this point, we re-cultured the cells, and when the cell confluence reached 50%, performed cell starvation treatment. DEME culture fluid was removed, and the NRK cells were rinsed three times with 1× EBSS and incubated in 1× EBSS for 0, 0.5, 1 and 2 h.

2.4. RNA-Seq Library Preparation and Sequencing

NRK cells were treated with EBSS for 0 or 2 h, respectively, collecting >1 × 10^7 cells at each time point and repeating the process three times. The NRK cell total RNAs were extracted by TRIeasyTM Total RNA Extraction Reagent (Shanghai Yeasen Biotechnology, Shanghai, China, 10606ES60), with the RNA concentrations from the cell samples measured with a Nanodrop 2000 spectrophotometer (Thermo Fisher Scientific, Waltham, MA, USA), the RNA quality measured with an ultraviolet–visible spectrophotometer (Merrler Toledo Company, Zurich, Switzerland, UV5) and the RNA integrity tested using an Agilent Technologies 2100 Bioanalyzer. Equal amounts of high-quality total RNA per sample were used to construct the RNA-seq libraries, with each RNA-seq library constructed with the VAHTS Stranded mRNA-seq Library Prep Kit for Illumina (Vazyme, Shanghai, China, NR602-02) and the library products sequenced on a HiSeq 4000 system (Illumina, San Diego, CA, USA). Finally, the RNA-seq raw data (ID: PRJNA1303382) were uploaded to the NCBI Sequence Read Archive (https://ncbiinsights.ncbi.nlm.nih.gov/tag/sra/, accessed on 20 August 2029).

2.5. Quantification and Analysis of RNA-Seq Data

For transcriptome data, the bowtie–tophat–cufflinks flow path was used for the assembly and quantification of the transcriptome data. The value of fragments per kilobase of exon model per million mapped fragments (FPKM) was recorded to estimate the gene mRNA expression levels. We then used the bioinformatics software Cuffdiff to screen for differentially expressed genes in the EBSS-induced autophagic cells. For gene ontology (GO)-based enrichment analysis, KEGG (Kyoto Encyclopedia of Genes and Genomes) enrichment analysis and heat map generation, we used the R language for data calculation and graph drawing, and for the protein–protein interaction (PPI) networks, we used the STRING database and R language for data mining. Considering the excessive number of differentially expressed genes, the samples were sorted by fold change values in descending order, selecting the top 27 candidate genes (fold change > 2.4, p-value < 0.05) for the subsequent experiments.

2.6. Immunoblotting Analysis

The protease (Roche, Basel, Switzerland, 4693116001) and phosphatase inhibitors (Roche, 4906837001) were dissolved in RIPA lysis buffer (Beyotime, Wuhan, China, P0013B), and the NRK cells were lysed with RIPA lysis buffer. Cell samples were mixed with SDS buffer and kept at 98 °C for 5 min, followed by protein separation by SDS-PAGE electrophoresis and transfer to PVFD membranes. The PVDF membranes were blocked for 2 h with 5% nonfat milk, then rinsed three times with TBST buffer. The primary and secondary antibodies were incubated with the membranes overnight at 4 °C, and the following day, the membranes were rinsed three times with TBST buffer. The Odyssey_CLx imaging system (LI-COR, Odyssey) was used to capture and analyze the immunoblotting results.

2.7. Immunofluorescence Microscopy Procedures

A total of 4×10^4 NRK-GFP-LC3 cells were inoculated into a confocal dish for 24 h. DEME culture fluid was removed, and the NRK cells were rinsed three times with 1× EBSS before being incubated in 1× EBSS for 0, 0.5, 1 and 2 h. After the processing at each time point was complete, the cell samples were photographed using a fluorescence confocal microscope.

2.8. RNA Interference

Cells were transfected with siRNAs (100 nM) using Lipofectamine RNAi Max (Invitrogen, Carlsbad, CA, USA, 13778150) for 48 h according to the manufacturer's instructions, and then treated with EBSS for 2 h. Immunoblotting analysis was performed as previously described, and the protein expression levels were quantified and analyzed using Image Studio software Ver.5.2 (LI-COR, Odyssey). Fluorescent images of cells were captured using an Olympus FV1000 (Olympus Corporation, Tokyo, Japan). Txnrd1 siRNA sense: CGGGAUAACAACAAAUGUUAUTT. Txnrd1 siRNA antisense: AUAACAUUUGUUGUUAUCCCGTT.

2.9. Analysis of Data

For RNA-seq analysis, the *p*-values were corrected using the FDR method.

The experimental data were analyzed by Student's *t*-test, with * $p < 0.05$ considered a significant difference. Each sample was produced in triplicate.

3. Results

3.1. EBSS-Induced Autophagy in NRK Cells

To detect the effect of autophagy induction by EBSS on NRK cells, the cells were treated with EBSS for 0 h, 0.5 h, 1 h and 2 h. Western blotting showed that the protein levels of LC3B-II increased with time and reached their maximum at 2 h (Figure 1A).Cell survival rates were also detected (Figure 1B), and we thus further investigated the numbers of GFP-LC3 puncta in EBSS-induced autophagic NRK-GFP-LC3 cells [14–17]. With the help of fluorescence microscopy, we found that NRK-GFP-LC3 cells treated with EBSS had increased numbers of GFP-LC3 puncta, and longer treatments had stronger inductive effects, with the maximum number reached at 2 h (Figure 1C,D). Taken together, these results demonstrated that EBSS could activate autophagy in NRK cells and that the LC3B-II protein and GFP-LC3 puncta levels reached their maximum after 2 h.

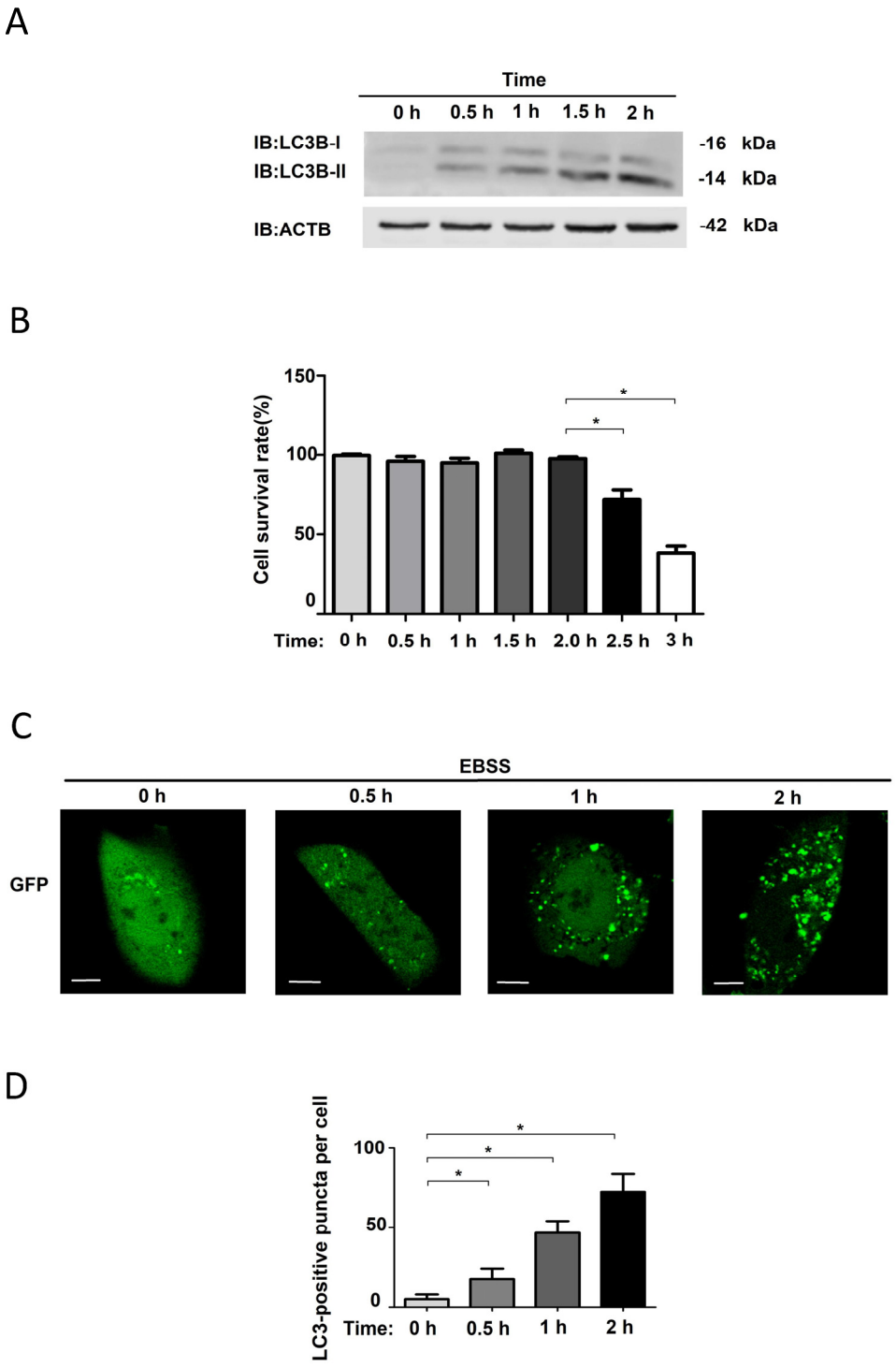

Figure 1. Autophagy is induced in NRK cells by EBSS. (**A**) NRK cells were incubated with EBSS for 0, 0.5, 1 and 2 h. LC3B-II protein levels were analyzed by immunoblotting. (**B**) NRK cells were incubated with EBSS, and cell survival rate was measured by the cck-8 kit. (**C**) NRK-GFP-LC3 cells were treated with EBSS for 0, 0.5, 1 and 2 h and images were captured by confocal microscope. Scale bar: 5 μm. (**D**) The average number of GFP-LC3 puncta per cell was counted in (**C**) at 0, 0.5, 1 and 2 h, respectively. GFP-LC3 puncta were quantified in ≥30 cells. *, $p < 0.05$.

3.2. Quantification and Analysis of RNA-Seq Data for EBSS-Induced Autophagic NRK Cells

From the above results, we found that 2 h of EBSS treatment efficiently induced autophagy in NRK cells. In this work, we hypothesized that there would be noticeable changes to the omics levels of proteins with regulatory functions in EBSS-induced au-

tophagy when cells were treated with EBSS. To fully excavate the functional proteins and probe the molecular changes during EBSS-induced autophagy, we used EBSS to treat NRK cells for 0 h and 2 h and applied next-generation sequencing to quantify the transcriptome data and collect gene expression levels (Figure 2).

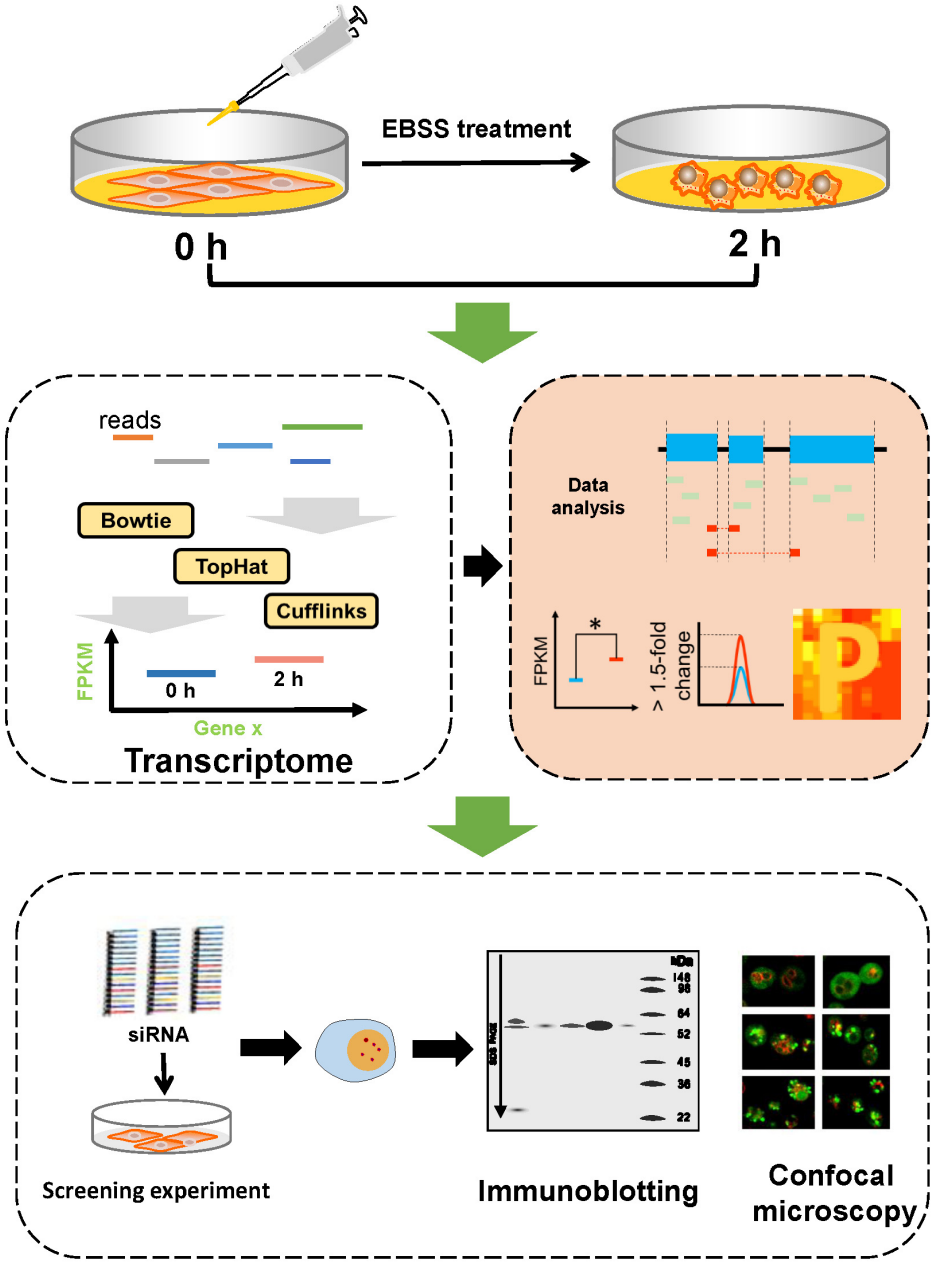

Figure 2. Experimental procedure of the study. The NRK cells were incubated for 0 and 2 h, and we then used next-generation sequencing technology to quantify the cell sample RNA-seq data. The bowtie–tophat–cufflinks flow path was used to analyze the transcriptome data. We used the bioinformatics software Cuffdiff to screen the differentially expressed genes in EBSS-induced autophagy. If the FPKM value of the treated group was significantly different from that of the control group, the gene was considered differential. Finally, we used gene knockdown technology, Western blotting and confocal microscopy to verify the prediction results. *, $p < 0.05$.

In our data, there were 11,852 genes mapped with at least one read (Table S1). From Figure 3A, it can be seen from the omics data that the density distribution of the genes was even, which reflects the absence of errors in the preparation and sequencing of the transcriptome samples. Volcano plots are a type of scatter plot that combine measures

of statistical significance (such as *p*-value) with the amplitude of variation in statistical tests, used here to quickly and intuitively identify datapoints that are significantly different. In Figure 3B, 509 genes are shown to be upregulated and 569 genes downregulated in cells treated for 2 h (|log2(fold_change)| > 1). Comparing gene transcription levels between the 2 h treatment group and 0 h treatment group, if the FPKM value of a gene in the treated group was significantly different from that of the control group (FPKM > 1, log2(fold_change) > 1, *p*-value < 0.05), it was considered differential. We found 470 genes that may have regulatory function (Table S2).

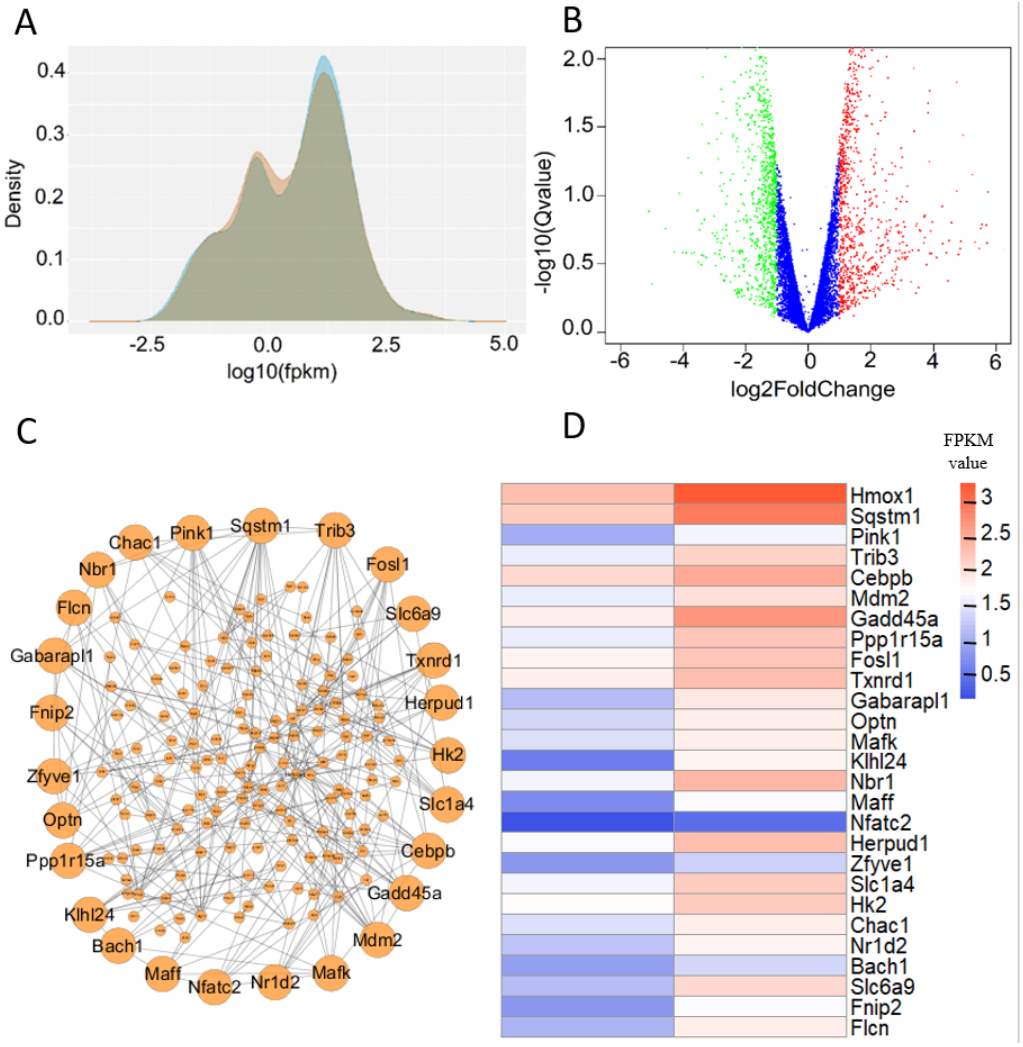

Figure 3. Quantitative analysis of transcriptome data. (**A**) The density distribution of all the genes in the transcriptome data. (**B**) Upregulated and downregulated genes. (**C**) Identified PPI networks. (**D**) The FPKM values of the 27 candidate genes at 0 h and 2 h in EBSS-induced autophagy.

Next, for a better understanding of the regulatory roles of these 470 genes, GO and KEGG enrichment analysis were performed, and numerous significantly enriched biological pathways were detected (*p*-value < 10^{-3}). Interestingly, we found that most of these signaling pathways were validated to be closely associated with autophagy (Figures 4 and 5), such as the responses to unfolded protein (GO:0006986) and topologically incorrect protein (GO:0035966), which have been reported to be crucial in autophagy. Moreover, responses to both oxygen levels (GO:0070482) and amino acid transport (GO:0006865) are known to participate in autophagy regulation.

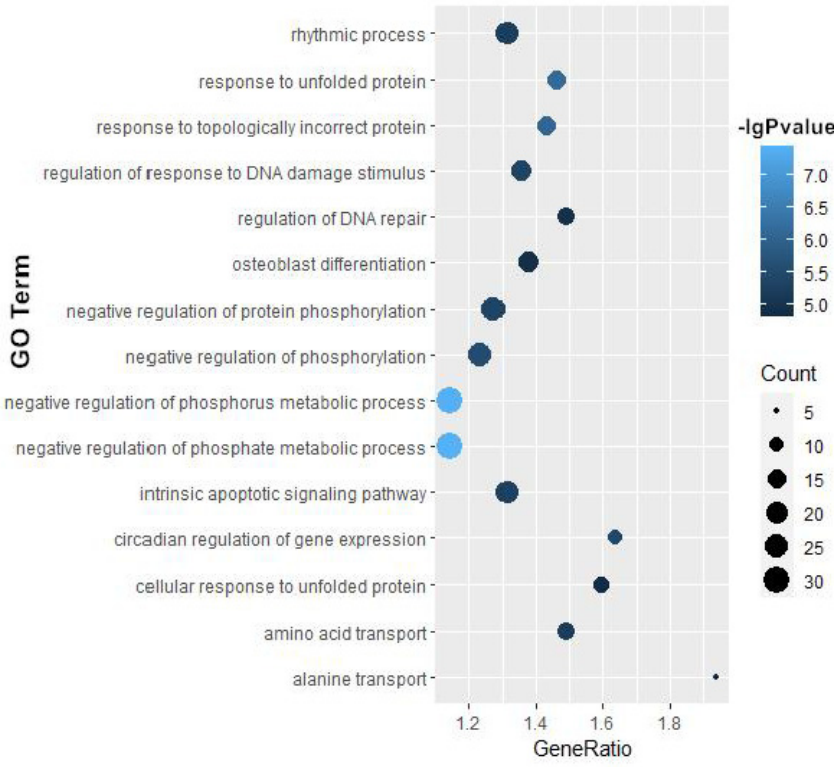

Figure 4. The GO-based enrichment results of biological processes.

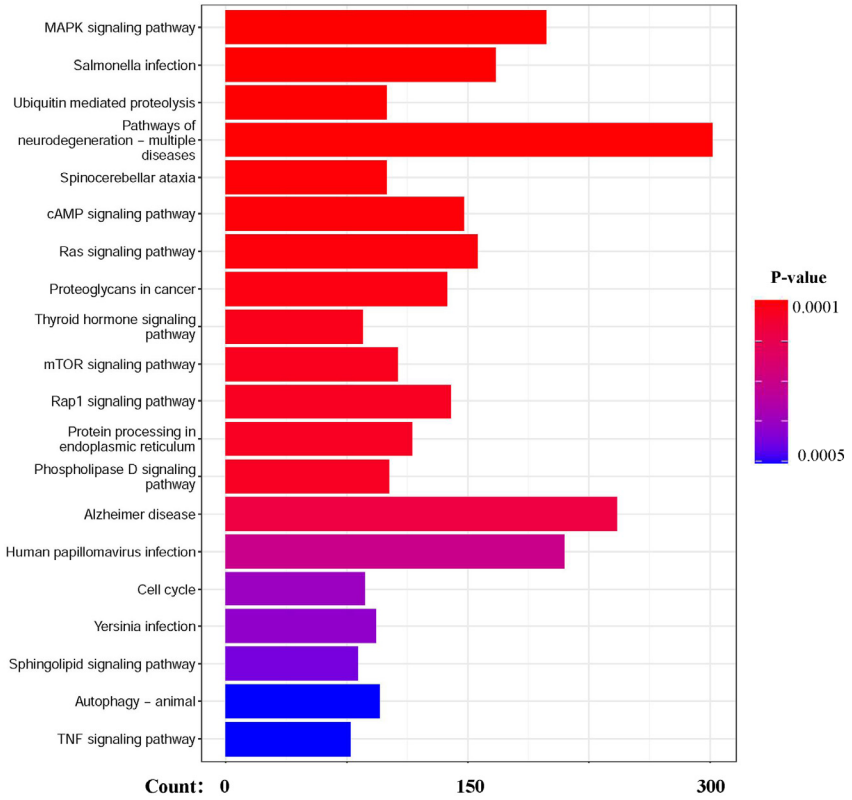

Figure 5. The KEGG-based enrichment results of biological processes.

Next, we explored the relationships between these proteins, making PPI networks, with the proteins with the most interaction effects shown in Figure 3C. Considering all the data analysis results, we choose the top 27 candidate genes (fold change > 2.4, p-value < 0.05) and examined their regulatory function in EBSS-induced autophagy (Figure 3D).

3.3. Validation of Regulatory Function of Candidate Proteins

With the help of next-generation sequencing technology and bioinformatics analysis, we choose 27 candidate genes and analyzed their function in EBSS-induced autophagy, further verifying our results using a small interfering RNA (siRNA) library designed with siRNA duplexes for each protein. The NRK cells were individually transfected with an siRNA for 48 h and then incubated with EBSS for 2 h before we collected the cell samples and detected LC3B-II protein levels by Western blot assay. Here, we also found a new gene, *Txnrd1*, that appeared to influence LC3B-II protein expression. To further confirm the function of TXNRD1 in EBSS-induced autophagy, we completed two additional siRNA-mediated knockdown experiments (Figure 6A), further investigating the numbers of GFP-LC3 puncta in NRK-GFP-LC3 cells by fluorescence microscopy and finding that *Txnrd1* knockdown reduced GFP-LC3 puncta numbers after 1 h and 2 h of culture in EBSS (Figure 6B), consistent with our knockdown experiments (Figure 6A).

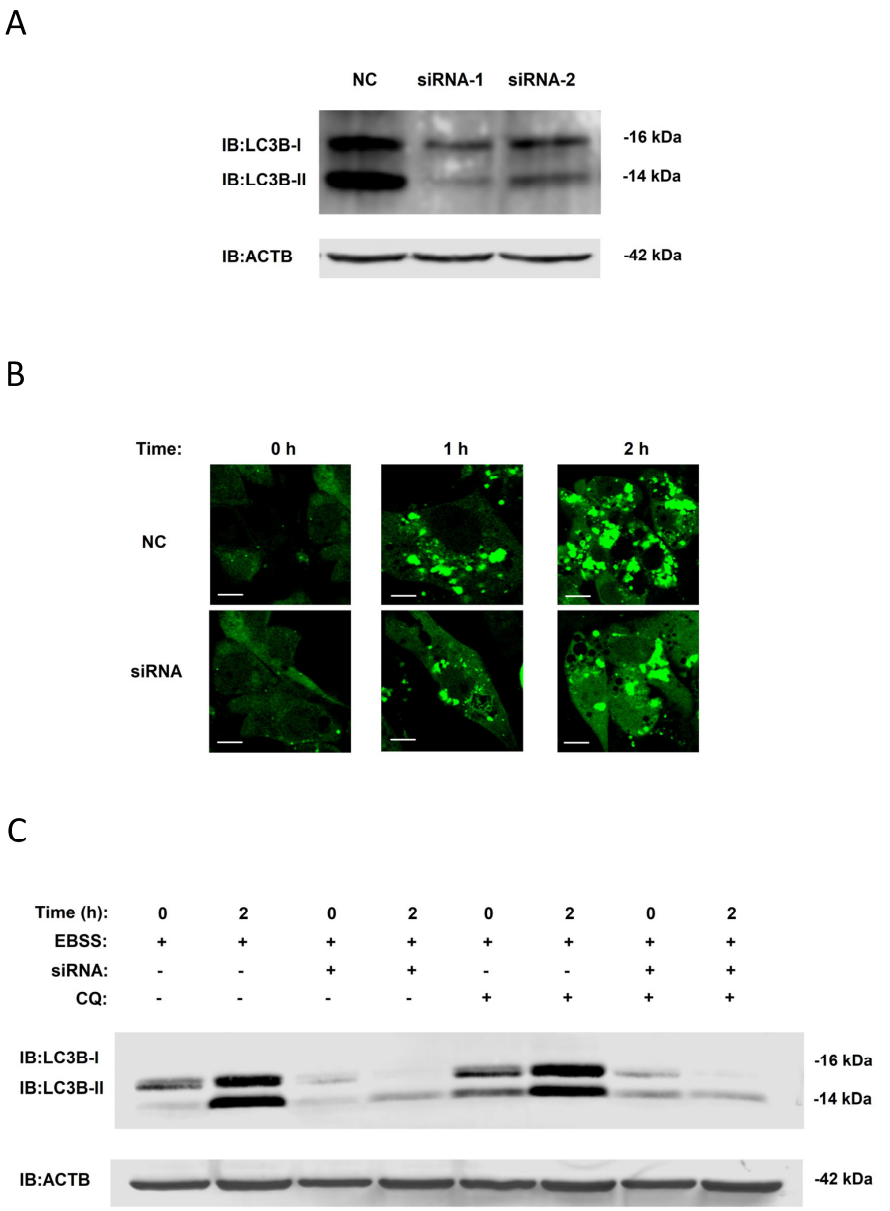

Figure 6. Validation of the regulatory function of proteins. (**A**) To further confirm the function of *Txnrd1* in EBSS-induced autophagy, siRNA-mediated knockdown experiments were performed of LC3-II and ACTB protein levels were measured by Western blot. (**B**) NRK-GFP-LC3 cells were individually transfected with specific siRNAs for 48 h and then treated with the EBSS for 0, 1 and 2 h.

DMSO was a negative control group. The images were captured by a confocal microscope. Scale bar: 5 μm. (**C**) NRK cells were incubated with siRNAs for 48 h and treated with CQ for 8 h followed by EBSS for 2 h. The LC3-II and ACTB protein levels were then measured by Western blot.

From the above results, we know that *Txnrd1* knockdown causes a decrease in LC3B-II expression. There may be two reasons for this decline: one is the inhibition of the activation of upstream autophagy, and the other is an improvement in downstream autophagy degradation. To address these issues, Chloroquine (CQ), an autophagy inhibitor, was added to the knockdown experimental system of EBSS-induced autophagy, and we found that its addition did not affect the significant decrease in intracellular LC3-II protein content (Figure 6C). It can be concluded that TXNRD1 plays a role in the autophagy activation process, via an unknown pathway, but not in the later stages of autophagy.

4. Discussion

EBSS has been used in many autophagy research projects, almost always as a positive control, but the details of the relationship between EBSS and autophagy are still not clear. In this study, we selected NRK cells as the study model, as they have low initial autophagy levels. One limitation of this study is that its central conclusions are mainly based on a single NRK cell line, and no confirmatory experiments on other cell lines were conducted. In future in-depth research, we will conduct more thorough verification.

We detected LC3B-II protein levels when the NRK cells were incubated with EBSS for 1 h and 2 h (Figure 1A) and found that these LC3B-II levels continuously increased over time, indicating that, during the formation of the autophagosome membrane, the LC3B precursor is being cleaved by ATG4, and the autophagosome is gradually forming; with the help of confocal microscopy, we also found that autophagy intensity reached its maximum at 2 h (Figure 1C,D). These two experimental results are mutually corroborative. Our results indicate that EBSS activated autophagy in NRK cells. Previous studies have shown similar results, with one study pointing out that EBSS starvation treatment could significantly increase the autophagosome numbers in nasopharyngeal carcinoma cells [18]. In the quest to explore the relationship between the liver and obesity, researchers have also found that EBSS could activate autophagy in mice liver cells [19].

As shown in Figure 1B, we found that after the cells were treated for 2 h, their survival rates significantly decreased, indicating that, after 2 h of EBSS treatment, autophagy reached its peak and autophagic death eventually occurred. In other studies, EBSS starvation treatment induced autophagy in pig fibroblast cells, with LC3B-II protein levels significantly increasing after 4 h [8]. In HeLa cells, autophagosome and autolysosome levels significantly increased when cells were incubated in EBSS medium for 1 h, with extremely significant increases at 4 h [20,21]. These different autophagy induction times in HBSS cells may be closely related to specific cell types.

Next-generation sequencing was used to obtain quantitative RNA-seq data for the cell samples incubated with EBSS at two time points (0 h and 2 h), a design derived from the results in Figure 1B, selecting the time point at which the autophagy effect was the strongest for analysis. However, this binary design may overlook dynamic transcriptional changes occurring earlier or later, resulting in the loss of information. Including an intermediate (e.g., 1 h) or longer (4 h) time point would be better, providing a more comprehensive picture.

With the help of RNA interference and Western blot assays, we found that the expression of a new gene, Txnrd1, influenced LC3B-II levels (Figure 6A), suggesting that the Txnrd1 functions to affect autophagy in cells. Not only that, but during the verification process, we also found several genes which have been reported as having regulatory functions and mechanisms during autophagy, including Gabarapl1 and Sqstm1. SQSTM1 is an

important marker protein in autophagy, playing several roles in autophagy regulation [11], with researchers finding that reducing SQSTM1 expression could significantly affect autophagy activation in cancer cells [22]. In addition, the GABARAP family is essential for phagophore initiation and autophagosome maturation [23], and the FLCN-GABARAP signaling pathway is associated with FNIP2, regulated by ULK1 [24]. In the face of this evidence, classical experimental methods can still uncover new clarifying information.

With the help of a confocal microscope, We observed that Txnrd1 expression was correlated with the number of GFP-LC3 puncta (Figure 6B), with mutually confirmatory experimental data. In the CQ experiment, we found that the addition of the autophagy inhibitor CQ did not affect the significant decrease in intracellular LC3-II protein content. Therefore, it can be concluded that Txnrd1 plays a role in autophagy activation, via an unknown pathway, but not in the later stages of autophagy. Coincidentally, scientists have also demonstrated that Txnrd1 plays a key role in ROS-mediated autophagy [25], a conclusion which supports our results.

TXNRD1 is one of the members of the selenoprotein family, with selenocysteine (Sec) as its common catalytic activity center, which comprises the main carriers of selenium for physiological functions [26]. Selenoproteins exist primarily in the form of redox enzymes and carry out very diverse functions integrally related to the development of diverse tumors, such as the regulation of cellular oxidative stress, immune function, ER stress, and autophagy [27,28]. In rat ovaries, rapamycin treatment has been shown to lead to an increase in transcriptional TXNRD1 level [29], and more importantly, one report clearly suggested the key role and potential interactions of the selenoproteins Txnrd1, Txnrd3, Selp, GPX2, Dio3 and Selr in ROS-mediated autophagy [25]. The mechanisms relating TXNRD1 to autophagy remain unclear, but according to the available literature, the selenoprotein family has complex interactions and regulatory relationships with cellular autophagy.

5. Conclusions

EBSS was one of the first autophagy inducers to be used experimentally, but there are almost no relevant omics data that reveal its autophagy-inducing mechanisms. In this study, a transcriptome data approach uncovered the regulatory roles of proteins in EBSS-induced autophagy, indicating that TXNRD1 plays a role in regulating EBSS-induced autophagy via an unknown pathway. However, the related regulation mechanisms of this protein need to be studied further. We hope that our bioinformatics analysis of transcriptome data will be helpful for those wishing to further elucidate the autophagy mechanisms of EBSS.

Supplementary Materials: The following supporting information can be downloaded at: https://www.mdpi.com/article/10.3390/biology14101373/s1. Table S1: An overview of data of each gene for RNA-seq; Table S2: The detailed results of 470 genes.

Author Contributions: Writing—original draft preparation and review, C.R.; validation, Y.L. and R.W. All authors have read and agreed to the published version of the manuscript.

Funding: The funding was provided by Natural Science Foundation of Henan (242300420500), Key Scientific Research Project Plan of Henan Higher Education Institutions (23A180023), Henan Province Science and Technology Tackling Plan Project (252102111148), Nanyang City Science and Technology Development Plan (2024KJGG0121), the PHD Scientific Research Foundation Project and Interdisciplinary Science Research Project, Nanyang Institute of Technology.

Informed Consent Statement: Not applicable.

Data Availability Statement: The original data presented in the study are openly available in the NCBI SRA database at https://dataview.ncbi.nlm.nih.gov/object/PRJNA1303382?reviewer=ml4bk1q4sjj8m70v06n19o0dto, accessed on 20 August 2029.

Conflicts of Interest: The authors declare no conflicts of interest.

Abbreviations

The following abbreviations are used in this manuscript:

EBSS	Earle's balanced salt solution
MTOR	mechanistic target of rapamycin kinase
NRK	normal rat kidney
LC3B	microtubule-associated protein 1 light chain 3 beta
ACTB	β-actin
FPKM	value of fragments per kilobase of exon model per million mapped fragments
GO	gene ontology
KEGG	Kyoto Encyclopedia of Genes and Genomes
PPI	protein–protein interaction
siRNA	small interfering RNA

References

1. Xie, Y.; Kang, R.; Sun, X.; Zhong, M.; Huang, J.; Klionsky, D.J.; Tang, D. Posttranslational modification of autophagy-related proteins in macroautophagy. *Autophagy* **2015**, *11*, 28–45. [CrossRef]
2. McEwan, D.G.; Dikic, I. The Three Musketeers of Autophagy: Phosphorylation, ubiquitylation and acetylation. *Trends Cell Biol.* **2011**, *21*, 195–201. [CrossRef] [PubMed]
3. Ohsumi, Y. Historical landmarks of autophagy research. *Cell Res.* **2014**, *24*, 9–23. [CrossRef] [PubMed]
4. Korah, J.; Canaff, L.; Lebrun, J.J. The Retinoblastoma Tumor Suppressor Protein (pRb)/E2 Promoter Binding Factor 1 (E2F1) Pathway as a Novel Mediator of TGFβ-induced Autophagy. *J. Biol. Chem.* **2016**, *291*, 2043–2054. [CrossRef] [PubMed]
5. Ruan, C.; Wang, C.; Gong, X.; Zhang, Y.; Deng, W.; Zhou, J.; Huang, D.; Wang, Z.; Zhang, Q.; Guo, A.; et al. An integrative multi-omics approach uncovers the regulatory role of CDK7 and CDK4 in autophagy activation induced by silica nanoparticles. *Autophagy* **2021**, *17*, 1426–1447. [CrossRef]
6. Gao, G.; Chen, W.; Yan, M.; Liu, J.; Luo, H.; Wang, C.; Yang, P. Rapamycin regulates the balance between cardiomyocyte apoptosis and autophagy in chronic heart failure by inhibiting mTOR signaling. *Int. J. Mol. Med.* **2020**, *45*, 195–209. [CrossRef]
7. Zhu, W.; Wang, X.; Zhou, Y.; Wang, H. C2-ceramide induces cell death and protective autophagy in head and neck squamous cell carcinoma cells. *Int. J. Mol. Sci.* **2014**, *15*, 3336–3355. [CrossRef]
8. Jiao, D.; Yang, Z.; Wang, L.; Hu, B.; Wang, J.; Xu, A.; Cheng, W.; Jia, B.; Qing, Y.; Zhao, H.-Y.; et al. Endogenous leptin promotes autophagy in EBSS-induced PFCs. *Anim. Cells Syst.* **2019**, *23*, 318–325. [CrossRef]
9. Mizushima, N.; Kuma, A.; Kobayashi, Y.; Yamamoto, A.; Matsubae, M.; Takao, T.; Natsume, T.; Ohsumi, Y.; Yoshimori, T. Mouse Apg16L, a novel WD-repeat protein, targets to the autophagic isolation membrane with the Apg12-Apg5 conjugate. *J. Cell Sci.* **2003**, *116 Pt 9*, 1679–1688. [CrossRef]
10. Klionsky, D.J.; Abeliovich, H.; Agostinis, P.; Agrawal, D.K.; Aliev, G.; Askew, D.S.; Baba, M.; Baehrecke, E.H.; A Bahr, B.; Ballabio, A.; et al. Guidelines for the use and interpretation of assays for monitoring autophagy in higher eukaryotes. *Autophagy* **2008**, *4*, 151–175. [CrossRef]
11. Klionsky, D.J.; Abdel-Aziz, A.K.; Abdelfatah, S.; Abdellatif, M.; Abdoli, A.; Abel, S.; Abeliovich, H.; Abildgaard, M.H.; Abudu, Y.P.; Acevedo-Arozena, A.; et al. Guidelines for the use and interpretation of assays for monitoring autophagy (4th edition)(1). *Autophagy* **2021**, *17*, 1–382. [CrossRef]
12. Cai, W.; Xiang, T.; Liu, X.; Fu, C. Multi-omics analysis reveals the role of the autophagy-related gene AGT in chemotherapy resistance in colorectal cancer and the therapeutic potential of its inhibitors. *Discov. Oncol.* **2024**, *15*, 674. [CrossRef] [PubMed]
13. Fan, Z.; Zhang, Y.; Yuan, L.; Gao, Y.; Tian, X.; Tian, J.; Wan, J.; Li, B.; Wang, X.; Wang, S.; et al. LARS1 lactylation inhibits autophagy by activating mTORC1 to promote podocytes injury in diabetic kidney disease. *Cell. Signal.* **2025**, *134*, 111955. [CrossRef] [PubMed]
14. Peng, D.; Ruan, C.; Fu, S.; He, C.; Song, J.; Li, H.; Tu, Y.; Tang, D.; Yao, L.; Lin, S.; et al. Atg9-centered multi-omics integration reveals new autophagy regulators in Saccharomyces cerevisiae. *Autophagy* **2021**, *17*, 4453–4476. [CrossRef]
15. Patterson, G.H.; Knobel, S.M.; Sharif, W.D.; Kain, S.R.; Piston, D.W. Use of the green fluorescent protein and its mutants in quantitative fluorescence microscopy. *Biophys. J.* **1997**, *73*, 2782–2790. [CrossRef]
16. Kimura, S.; Noda, T.; Yoshimori, T. Dissection of the autophagosome maturation process by a novel reporter protein, tandem fluorescent-tagged LC3. *Autophagy* **2007**, *3*, 452–460. [CrossRef]

17. Rekas, A.; Alattia, J.R.; Nagai, T.; Miyawaki, A.; Ikura, M. Crystal structure of venus, a yellow fluorescent protein with improved maturation and reduced environmental sensitivity. *J. Biol. Chem.* **2002**, *277*, 50573–50578. [CrossRef]
18. Zhu, Q.; Zhang, Q.; Gu, M.; Zhang, K.; Xia, T.; Zhang, S.; Chen, W.; Yin, H.; Yao, H.; Fan, Y.; et al. MIR106A-5p upregulation suppresses autophagy and accelerates malignant phenotype in nasopharyngeal carcinoma. *Autophagy* **2021**, *17*, 1667–1683. [CrossRef]
19. Zhang, Z.; Qian, Q.; Li, M.; Shao, F.; Ding, W.-X.; Lira, V.A.; Chen, S.X.; Sebag, S.C.; Hotamisligil, G.S.; Cao, H.; et al. The unfolded protein response regulates hepatic autophagy by sXBP1-mediated activation of TFEB. *Autophagy* **2021**, *17*, 1841–1855. [CrossRef]
20. Chu, Y.; Kang, Y.; Yan, C.; Yang, C.; Zhang, T.; Huo, H.; Liu, Y. LUBAC and OTULIN regulate autophagy initiation and maturation by mediating the linear ubiquitination and the stabilization of ATG13. *Autophagy* **2021**, *17*, 1684–1699. [CrossRef]
21. Tian, S.; Jin, S.; Wu, Y.; Liu, T.; Luo, M.; Ou, J.; Xie, W.; Cui, J. High-throughput screening of functional deubiquitinating enzymes in autophagy. *Autophagy* **2021**, *17*, 1367–1378. [CrossRef] [PubMed]
22. Ren, F.; Shu, G.; Liu, G.; Liu, D.; Zhou, J.; Yuan, L.; Zhou, J. Knockdown of p62/sequestosome 1 attenuates autophagy and inhibits colorectal cancer cell growth. *Mol. Cell. Biochem.* **2014**, *385*, 95–102. [CrossRef] [PubMed]
23. Galluzzi, L.; Baehrecke, E.H.; Ballabio, A.; Boya, P.; Bravo-San Pedro, J.M.; Cecconi, F.; Choi, A.M.; Chu, C.T.; Codogno, P.; Colombo, M.I.; et al. Molecular definitions of autophagy and related processes. *Embo. J.* **2017**, *36*, 1811–1836. [CrossRef]
24. Dunlop, E.A.; Seifan, S.; Claessens, T.; Behrends, C.; Kamps, M.A.; Rozycka, E.; Kemp, A.J.; Nookala, R.K.; Blenis, J.; Coull, B.J.; et al. FLCN, a novel autophagy component, interacts with GABARAP and is regulated by ULK1 phosphorylation. *Autophagy* **2014**, *10*, 1749–1760. [CrossRef]
25. Tan, S.; Zheng, Z.; Liu, T.; Yao, X.; Yu, M.; Ji, Y. Schisandrin B Induced ROS-Mediated Autophagy and Th1/Th2 Imbalance via Selenoproteins in Hepa1-6 Cells. *Front. Immunol.* **2022**, *13*, 857069. [CrossRef]
26. Jiayong, Z.; Shengchen, W.; Xiaofang, H.; Gang, S.; Shiwen, X. The antagonistic effect of selenium on lead-induced necroptosis via MAPK/NF-κB pathway and HSPs activation in the chicken spleen. *Ecotoxicol. Environ. Saf.* **2020**, *204*, 111049. [CrossRef]
27. Zhang, Y.; Xu, Y.; Chen, B.; Zhao, B.; Gao, X.J. Selenium Deficiency Promotes Oxidative Stress-Induced Mastitis via Activating the NF-κB and MAPK Pathways in Dairy Cow. *Biol. Trace Elem. Res.* **2022**, *200*, 2716–2726. [CrossRef]
28. Chi, Q.; Zhang, Q.; Lu, Y.; Zhang, Y.; Xu, S.; Li, S. Roles of selenoprotein S in reactive oxygen species-dependent neutrophil extracellular trap formation induced by selenium-deficient arteritis. *Redox Biol.* **2021**, *44*, 102003. [CrossRef]
29. Madden, J.A.; Thomas, P.Q.; Keating, A.F. Phosphoramide mustard induces autophagy markers and mTOR inhibition prevents follicle loss due to phosphoramide mustard exposure. *Reprod. Toxicol.* **2017**, *67*, 65–78. [CrossRef]

Disclaimer/Publisher's Note: The statements, opinions and data contained in all publications are solely those of the individual author(s) and contributor(s) and not of MDPI and/or the editor(s). MDPI and/or the editor(s) disclaim responsibility for any injury to people or property resulting from any ideas, methods, instructions or products referred to in the content.